Food Biophysics

Cinnamon essential oil encapsulated into a fish gelatin-bacterial cellulose nanocrystals complex and active films thereof

--Manuscript Draft--

Manuscript Number:	FOBI-D-21-00126R2
Full Title:	Cinnamon essential oil encapsulated into a fish gelatin-bacterial cellulose nanocrystals complex and active films thereof
Article Type:	Original Research
Keywords:	antimicrobial; coatings; permeability; release; shelf life; wettability
Corresponding Author:	Stefano Farris Università degli Studi di Milano: Universita degli Studi di Milano Milan, ITALY
Corresponding Author Secondary Information:	
Corresponding Author's Institution:	Università degli Studi di Milano: Universita degli Studi di Milano
Corresponding Author's Secondary Institution:	
First Author:	Mahsa Sadat Razavi
First Author Secondary Information:	
Order of Authors:	Mahsa Sadat Razavi
	Abdollah Golmohammadi
	Ali Nematollahzadeh
	Cesare Rovera
	Stefano Farris
Order of Authors Secondary Information:	
Funding Information:	
Abstract:	In this study, cinnamon essential oil (CEO) nanocapsules were stabilized by means of bacterial cellulose nanocrystals (BCNCs) and encapsulated using fish gelatin as the main polymer phase. Emulsions were prepared at pH 5 using different CEO concentrations (0.03, 0.06, 0.12, 0.24, 0.36, and 0.48% v/w) and a fixed amount of fish gelatin (3% w/w) and BCNCs (0.06% w/w). The controlled release of the essential oil was assessed by release studies, which revealed that the higher the CEO concentration, the lower the release rate of CEO. In addition, modelling of experimental data using five different equations showed that the best fitting was obtained for the Korsmeyer-Peppas model, according to which the CEO release obeyed a non-Fickian behavior. Films obtained from the same formulations were characterized in terms of optical properties (light transmittance and haze), surface wettability, barrier (oxygen, carbon dioxide, and water vapor transmission rates) and mechanical properties. It was observed that an increased amount of CEO in the films did not significantly affect both transparency and haze, while it yielded an increase in surface hydrophobicity (~ 120% increase in water contact angle over the control) and elongation. Finally, the barrier performances of films against O2, CO2, and water vapor suggest a potential application of CEO/GelA-BCNC matrices as antimicrobial layers (in the form of coatings deposited on plastic films or directly on food) in living foods that have a respiratory metabolism, such as modified atmosphere-packaged crustaceans and mollusks as well as fruits and vegetables.

Cinnamon essential oil encapsulated into a fish gelatin-bacterial cellulose nanocrystals complex and active films thereof

Mahsa Sadat Razavi[1], Abdollah Golmohammadi[1,*], Ali Nematollahzadeh[2], Cesare Rovera[3], Stefano Farris[3*]

[1] *Department of Biosystems Engineering, University of Mohaghegh Ardabili, P.O. Box 179, Ardabil, Iran*

[2] *Department of Chemical Engineering, University of Mohaghegh Ardabili, P.O. Box 179, Ardabil, Iran*

[3] *DeFENS, Department of Food, Environmental and Nutritional Sciences, Food Packaging Lab, University of Milan, via Celoria 2 – I-20133 Milan, Italy*

***Corresponding authors**

Tel.: +39 0250316805; Fax: +39 0250316672

Email address: stefano.farris@unimi.it (S. Farris)

Tel.: +98 04515517500; Fax: +98 04515520567

Email address: golmohammdi1342@gmail.com (A. Golmohammadi)

Abstract

In this study, cinnamon essential oil (CEO) nanocapsules were stabilized by means of bacterial cellulose nanocrystals (BCNCs) and encapsulated using fish gelatin as the main polymer phase. Emulsions were prepared at pH 5 using different CEO concentrations (0.03, 0.06, 0.12, 0.24, 0.36, and 0.48% v/w) and a fixed amount of fish gelatin (3% w/w) and BCNCs (0.06% w/w). The controlled release of the essential oil was assessed by release studies, which revealed that the higher the CEO concentration, the lower the release rate of CEO. In addition, modelling of experimental data using five different equations showed that the best fitting was obtained for the Korsmeyer-Peppas model, according to which the CEO release obeyed a non-Fickian behavior. Films obtained from the same formulations were characterized in terms of optical properties (light transmittance and haze), surface wettability, barrier (oxygen, carbon dioxide, and water vapor transmission rates) and mechanical properties. It was observed that an increased amount of CEO in the films did not significantly affect both transparency and haze, while it yielded an increase in surface hydrophobicity (~ 120% increase in water contact angle over the control) and elongation. Finally, the barrier performances of films against O_2, CO_2, and water vapor suggest a potential application of CEO/GelA-BCNC matrices as antimicrobial layers (in the form of coatings deposited on plastic films or directly on food) in living foods that have a respiratory metabolism, such as modified atmosphere-packaged crustaceans and mollusks as well as fruits and vegetables.

Keywords: antimicrobial; coatings; permeability; release; shelf life; wettability

1. Introduction

Films and coatings from biodegradable polymers are an effective alternative to the conventional oil-based polymers that are used in the food packaging sector, especially from an environmental perspective [1–3]. Over the years, researchers have demonstrated that many biopolymers, mainly belonging to the realms of polysaccharides and proteins, can be virtually used to produce films and coatings. However, some critical drawbacks make their practical use difficult or restricted to small niches. This is the case, for example, with films and coatings obtained from gelatin. This protein has been considered a valid alternative to synthetic polymers, due to its biodegradability, biocompatibility, high processability, excellent film-forming characteristics, adhesiveness, and good barrier properties toward gases, oils, volatile compounds, and UV light [4–6]. However, gelatin, as many other biopolymers, exhibits high water sensitivity and low mechanical properties, especially compared to polymers of fossil origin [7, 8]. For these reasons, gelatin films have been proposed as a promising 'green' solution for low-to-intermediate water activity foods [9–12]. Among gelatins of different origins, fish gelatin is an alternative to mammalian gelatin, especially with respect to the risk associated with the bovine spongiform encephalopathy (BSE) epidemics and foot and mouth diseases (FMD) [13]. In addition, fish gelatin meets religious and moral concerns, such as kosher and halal requirements [14, 15]. Expanding the use of gelatin films and coatings can be achieved by increasing their multifunctionality. For example, the incorporation of active compounds such as plant essential oils (EOs) can provide new active (e.g., antimicrobial and antioxidant) features while possibly improving the water vapor resistance of the films. Different EOs have been embedded in gelatin films, such as oregano [16], cinnamon [17], mint [18], bergamot, kaffir lime, lemon, and lime [19].

Stable nanoemulsions of cinnamon essential oil (CEO) in water were obtained using fish gelatin and bacterial cellulose nanocrystals (BCNCs) [20]. Gelatin, because of its emulsifying

properties, allowed to form a continuous layer around CEO nanodroplets, thus stabilizing the emulsion by both a reduction of the interfacial tension and acting as a physical barrier to coalescence. BCNCs were instead used to form a cage-like configuration around the CEO-GelA droplets, contributing to the stability of the emulsion by preventing gravitational separation of CEO droplets (i.e., creaming).

In this study, we have explored the potential use of the CEO-GelA/BCNC nanoemulsions for the generation of biopolymer films for active food packaging applications. Cinnamon essential oil has been widely used in active packaging due to its antimicrobial and antioxidant properties [21–23]. The effectiveness of antimicrobial films is determined partially by the diffusion and release behavior of active molecules within or out of polymeric film matrix [7]. For this reason, we first characterized the release kinetics of the encapsulated CEO in a food simulant, assuming the potential use of the active films for, e.g., seafood (fish, crustaceans and mollusks). We then characterized active films in terms of barrier (against oxygen, carbon dioxide, and water vapor), optical (transparency and haze), and wettability properties.

2. Materials and Method

2.1. Materials

All the chemicals and reagents used in this study for the CEO-GelA/BCNC nanoemulsion preparation were the same as in our previous work [20]. Briefly, fish gelatin was obtained from Weishardt (Graulhet, France), whereas cinnamon (*Cinnamomum zeylanicum*) bark EO was purchased from Plant Therapy Essential Oils Corporate (Twin Falls, USA). The production of BC was done according to the static fermentation protocol as reported elsewhere [24]. Sulfuric acid (99% v/v), ethanol (96% v/v), and dialysis tubing cellulose membrane (12 kDa, average flat width 43 mm) were all purchased from Sigma-Aldrich-Merck (Milano, Italy).

2.2. CEO-GelA/BCNC emulsion preparation

The preparation of the CEO-GelA/BCNC emulsions was performed according to the procedure reported by Razavi et al. [20]. In a first step, BCNCs were obtained from the parental BC by acid hydrolysis using sulfuric acid and adjusting the pH to 5 by dialysis. In a second step, BCNCs-stabilized CEO emulsions at different concentrations were obtained by ultrasonication. Finally, BCNCs-stabilized CEO droplets were encapsulated using fish gelatin, which acted as a true surfactant adsorbed onto the oil surface fully covering the CEO nanodroplets [20]. The final CEO-GelA/BCNC emulsion included BCNCs and gelatin at 0.06% w/w and 3% w/w concentration, respectively, while the final concentrations of CEO were 0.03 (coded as T1G), 0.06 (T2G), 0.12 (T3G), 0.24 (T4G), 0.36 (T5G), and 0.48 (T6G) % (v/w).

2.3. Active films preparation

CEO-GelA/BCNC active films were prepared by pouring 6.5 g of each emulsion into a Petri dish (10 cm diameter) and drying at 23 ± 1 ºC and 50 ± 2.5 % relative humidity (RH) for 48 h. Then, the films were peeled off from the Petri dishes and put in a desiccator at 23 ± 1 ºC and 0% RH for at least one week before being analyzed.

2.4. In vitro release kinetics of CEO from CEO-GelA/BCNC emulsions

The release kinetics of CEO from the CEO-GelA/BCNC emulsions were determined according to the procedure proposed by Campos et al. [25] and Silva et al. [26] with slight modifications. Briefly, 2 mL of each emulsion was put in cellulose dialysis tubes (12 kDa) and then immersed in a beaker containing 100 mL of ethanol/water (20%, w/w) solution as a food simulant [27]. In addition, ethanol was used to minimize aggregation and make CEO release uniform across the dialysis tube [28]. The beaker was put on a magnetic stirrer with a gentle

speed (100 rpm) at room temperature (23 ± 1 ºC). At predetermined time intervals (0-7 h), 1 mL of external medium was taken and its absorbance at 287 nm measured spectrophotometrically using a Lambda 650 UV–visible spectrophotometer (PerkinElmer Inc., Waltham, USA). The absorbance at 287 nm was recorded and inserted into the regression equation of the standard curve [20], so that the CEO concentration was eventually gathered. To keep the volume of the food simulant constant throughout the experiment, 1 mL of fresh medium was replaced after each sampling. Zero-order, first-order, Higuchi, Hixson-Crowell, and Korsmeyer-Peppas mathematical models were fitted to the experimental release data to obtain a clear understanding of the mechanism underlying the CEO release [29, 30].

2.5. Film properties

2.5.1. Thickness

The thickness of CEO-GelA/BCNC films was measured by a digital micrometer to the nearest 0.001 mm (Mitutoyo, QuantuMike, Data output IP65, Serial No. 293-180, Mitutoyo Corp, Japan). For each sample, 10 replicates from random locations were taken and averaged.

2.5.2. Haze and transparency

The measurement of both haze and transparency was performed spectrophotometrically, using a Lambda 650 spectrophotometer (PerkinElmer, Waltham, MA, USA). Haze was determined according to ASTM D1003 within the wavelength range 380–780 nm, using a 150 mm integrating sphere that allowed to trap the diffuse transmitted light. Transparency was measured in accordance with ASTM D1746, according to which transparency is measured as specular transmittance—i.e., the transmittance value obtained when the transmitted radiant flux includes only the light transmitted in the same direction as that of the incident flux at a 550 nm wavelength [31]. For both haze and transparency, final data are the average of three replicates.

2.5.3. Wettability

An optical contact angle apparatus (OCA 15 Plus - Data Physics Instruments GmbH, Filderstadt, Germany) was used to determine the wettability of CEO-GelA/BCNC films in the form of rectangular specimens (5 × 1 cm^2). The equilibrium contact angle of water in air (θ, °) was measured by gently dropping a droplet of 2.0 ± 0.5 µL of Milli-Q water (18.3 MV cm) onto the substrate at 23 ± 1 °C and 50 ± 2% RH [32]. The software SCA 20 (Data Physics Instruments GmbH, Filderstadt, Germany) was used for data acquisition and contact angle measurement.

2.5.4. Water vapor, O_2, and CO_2 barrier properties

The barrier properties of CEO-GelA/BCNC films against oxygen, carbon dioxide, and water vapor were measured using a TotalPerm permeability analyzer (Extrasolution Srl, Capannori, Italy) equipped with an electrochemical sensor (for oxygen detection) and an infrared sensor (for carbon dioxide and water vapor measurements). The XS Pro software (Extrasolution Srl, Capannori, Italy) was used for data acquisition and analysis. CEO-GelA/BCNC films were sandwiched between two aluminum-tape masks, allowing a surface of 2.01 cm^2 to be exposed to the permeation. The oxygen transmission rate (OTR, mL m^{-2} 24 h^{-1}) and carbon dioxide transmission rate (CO_2TR, mL m^{-2} 24 h^{-1}) were determined according to the standard method of ASTM F1927 and ASTM F2476, with a carrier flow (N_2) of 10 mL min^{-1} at 23 °C and relative humidity (RH) of both 0% and 50% and with 1 atm pressure difference on the two sides of the specimen. Water vapor transmission rate (WVTR) (g m^{-2} 24 h^{-1}) was determined using the standard method ASTM F1249, with a carrier flow (N_2) of 10 mL min^{-1}. Measurements were performed at 23 °C and 50 % RH, which is the humidity gradient between the two semi-chambers between which the sample was mounted. Each OTR, CO_2TR, and WVTR value was from three replicates.

2.5.5. Mechanical properties

Tensile strength (TS), elongation at break (EAB), and Young's (elastic) modulus (YM) were measured using an Instron Universal Testing Machine STM-20 (Norwood, USA), according to the ASTM standard method D882. Sample films were cut into 60 × 20 mm^2 strips. The film samples were mounted between the two grips with an initial separation of 5.0 cm. The cross-head speed was constant at 1.0 mm/s. Each measurement comes from at least 5 replicates.

3. Results and Discussion

3.1. Release kinetics

The release rate of an active compound from a packaging system is of great importance to understanding the mechanism underlying the release process as well as to achieving a sustained release, possibly throughout the shelf life of the packaged food. A quantitative analysis of the release rate can be done using mathematical models that describe the release of the active compound (M) as a function of time (t) so that $M = f(t)$. In this work, the release of CEO from GelA/BCNC nanocapsules was investigated using the zero-order, first-order, Higuchi, Hixson-Crowell, and Korsmeyer-Peppas mathematical models (Table 1).

The zero-order model assumes that the release takes place at a constant rate because no disaggregation of the encapsulating matrix occurs over time [33]. The first-order model is usually applied for water-soluble active compounds encapsulated in porous matrices [34]. The Higuchi model is one of the most widely used in dealing with drug delivery problems [35]. The Higuchi model has been advantageously used to describe the release of both water-soluble and low-solubility molecules incorporated in semisolid and/or solid matrices [36]. The Hixson-Crowell model assumes that the surface area of a spherical particle incorporating an active molecule is proportional to the cube root of its volume. This model is used to describe the release by dissolution, assuming that the surface factors of spherical particles are constant if

the dissolution is constant over the entire system [33]. Finally, the Korsmeyer–Peppas model is used to investigate the transport mechanism of an active molecule through a polymer matrix. The *n* exponent in the Korsmeyer–Peppas equation is indicative of different release mechanisms of the active molecule from a polymeric system [37, 38]. More specifically, *n* allows one to distinguish between Fickian (diffusion-guided) and non-Fickian (other mechanisms such as water swelling of the polymer) release from polymeric materials of different shapes (Table 2).

In this study, the experimental release data were fitted with the above equations so that the release rate constants were calculated from the slope of the appropriate plots (Table 1), with the exception of the Korsmeyer-Peppas equation, whereby the release rate constant (K_{KP}) was the antilog of the intercept of the straight line equation obtained by the appropriate plot and the release exponent *n* was the slope of the same straight plot. For all the equations, the regression coefficient (or coefficient of determination, R^2) was calculated by linear regression analysis and used as an indicator of the best fitting. Both release rate constants and the regression coefficient are summarized in Table 3, whereas the experimental data and fits of the above mathematical models are displayed in Fig. S1 in the Supporting Information.

The release of CEO from the GelA/BCNC nanocapsules obtained at pH 5 was monitored over a 420-minute temporal window. As shown in Fig. 1, the larger part of CEO was released within the first 30 minutes, after which a sustained release occurred. The same trend was observed for the release of mint essential oil and cinnamon essential oil from micro- and nanocapsules in alcoholic aqueous food models [39–41]. This behavior is often observed for encapsulated systems, and the initial burst release of the EO is associated with the EO located in the outermost region of the capsule [42]. After 420 minutes, CEO release reached 55.68, 59.44, 63.33, and 67.85% of the total amount present in the emulsions for the T6G, T5G, T4G, and T3G formulations, respectively. Interestingly, the maximum and minimum release were

observed for the lowest and highest concentrations of CEO (T3G and T6G, respectively), plausibly due to the lower size of the nanocapsules with a lower amount of CEO, which implies a higher surface-to-volume (S/V) ratio compared to those of the biggest particles.

While all the models fitted satisfactorily the experimental data ($R^2 > 0.93$), the best fitting was obtained for the Korsmeyer-Peppas model, especially for the formulations containing the highest amount of CEO (T5G and T6G) (Table 3). According to the n values calculated for the four formulations from the Korsmeyer–Peppas model ($0.621 < n < 0.802$), it can be concluded that the CEO release obeyed a non-Fickian behavior—i.e., it followed an anomalous transport type of diffusional release, typical for both diffusion- and swelling-controlled drug releases [38]. More specifically, it is plausible that the release of CEO from the GelA/BCNC nanocapsules was governed by not only diffusion but also other mechanisms such as degradation and/or erosion of the capsules, likely due to the disassembly of BCNCs and swelling/dissolution of the GelA network. This finding may explain the sustained release over time of CEO from the encapsulated systems, making films thereof a potential solution for the development of a controlled-release active packaging system.

3.2. Thickness measurement

The thickness of active films is shown in Table 4. The addition of CEO did not bring about any statistically significant difference between the different formulations, in contrast to the observations made by Wu et al. [43], who reported a slight increase in the thickness of fish gelatin films when the concentration of CEO increased. This observation was explained in terms of the increased free volume of the films upon the addition of the essential oil.

3.3. Light transmittance and haze

The total light transmittance and haze values of films loaded with different CEO amounts are shown in Table 2. The light transmittance of films did not decrease significantly upon the addition of the essential oil. That the decrease in light transmittance in our study was very limited (which explains the not statistically significant difference between formulations) owes to our consideration of the total transmittance, which accounts for both specular and diffused light. In other words, the total transmittance values suggest that approximately 90% of incident light passed through the CEO-GelA/BCNC films, irrespective of the amount of light diffused or transmitted specularly. For this reason, to highlight the influence of the composition on the transparency of the films, we considered the haze of the films.

Haze represents by the amount (as %) of light transmitted across the sample that light deviates by more than an angle of 2.5° from the original direction of the incident light. From a practical point of view, haze is important because it is responsible for the reduction in the contrast between objects viewed through a specimen (the so-called 'see-through property' of materials) [44]. As can be seen in Table 4 and Fig. S2 in the Supporting Information, haze increased significantly moving from the formulation T1G to the formulation T6G. A decrease in transparency for films loaded with essential oils is expected in consideration of the scattering effect of the incident light by the oil droplets dispersed in the main polymer phase. This was confirmed by the observations of Tongnuanchan et al. [19] and Yao et al. [45], who reported a decrease in transparency for fish skin gelatin films incorporated with citrus EO and gelatin-chitosan films supplemented with D-Limonene. From a practical point of view, the haze values recorded in our study for all the formulations were below a 3% value, which is the threshold to guarantee an adequate display of the product inside the package [46].

3.4. Wettability

In the food packaging sector, the use of the contact angle technique especially pertains to the characterization of plastics because it allows for gathering thermodynamic information on a film surface and hence predicting the film behavior toward converting operations such as coating, printing, and lamination. In more recent years, contact angle analysis has been extended to biopolymer films and coatings, especially to investigate phenomena such as sorption and absorption that can dramatically affect deleterious phenomena (e.g., the formation of biofilms and microbial spoilage) [47].

Fig. 2 shows the water contact angle (θ) of GelA/BCNC films with different CEO concentrations. Control films (i.e., GelA/BCNC films without CEO) exhibited $\theta \sim 78°$, in line with the recent work by Li et al. [48]. The addition of CEO led to a statistically significant difference between GelA/BCNC films and all CEO-GelA/BCNC films. More specifically, in the presence of the essential oil, the active films had $\theta > 90°$, indicating that the surface properties shifted from hydrophilic to hydrophobic ones [49]. Similar results were reported by Hosseini et al. [16] for oregano oil in gelatin/chitosan films, Yao et al. [45] for gelatin/chitosan films incorporated with D-limonene, Scartazzini et al. [18] for gelatin films supplemented with mint EO, and Li et al. [48] for gelatin films loaded with thymol.

3.5. Water vapor, O_2, and CO_2 transmission rates (WVTR, O_2TR, CO_2TR)

The barrier properties against oxygen, carbon dioxide, and water vapor were assessed for the formulations T3G and T4G—that is, the GelA/BCNC films incorporating CEO at a concentration of 0.12 v/w % and 0.24 v/w %, respectively. We decided to focus only on these two formulations because they represent a good compromise between functional properties (releasing-behavior, optical, and surface properties) and the negative sensory impact possibly arising from higher CEO concentrations. OTR, CO_2TR, and WVTR of T3G and T4G CEO-

GelA/BCNC films are reported in Table 5. Two RH levels of 0 and 50% were used to test the gas barrier properties of the films.

Regardless of the amount of CEO loaded in the films, an increase in RH led to a dramatic increase of the gas permeability insomuch as the CO_2TR at 50% RH was well above the instrumental detection limit. These results can be attributed to the hydrophilic character of fish gelatin, which swells due to moisture uptake. In addition, gelatin films under dry conditions are in a glassy state, whereas the molecular organization shifts to a rubbery state after the adsorption of water molecules. In the rubbery state, the gas permeation is higher because of an increased free volume at the intermolecular level, owing to the plasticizing effect of water molecules, which reduces the transition temperature of gelatin and changes the system state from glassy to rubbery [50, 51]. The same considerations can be extended to the addition of CEO. In increasing the amount of CEO from 0.12 v/w % to 0.24 v/w % (i.e., moving from the formulation T3G to the formulation T4G), both OTR and CO_2TR increased correspondingly, confirming that essential oils have a plasticizing effect similar to that seen for water molecules. In particular, OTR increased by 3.7 times at 0% RH and by 12 times at 50% RH, moving from the formulation T3G to the formulation T4G. CO_2TR increased by 2.7 times at 0% RH when the CEO concentration was doubled (from 0.12 v/w % to 0.24 v/w %).

Finally, a reduction in WVTR occurred in increasing the amount of CEO incorporated in the films. This observation can be firstly attributed to the hydrophobic nature of CEO, which increases the repellency of water vapor on a film surface. In addition, CEO droplets entrapped in a biopolymer network create a twisting pathway for water vapor, hence slowing down the diffusion of the molecules across the film. Similar results were obtained for fish gelatin films incorporated with CEO nanoliposomes [43]. The authors reported that the results might have owed to the better interaction of the hydrocolloid gelatin and polar-head groups positioned in

the external membrane of nanoliposomes. This interaction led to an even dispersion of nanoliposomes in the film, which allowed for the reduction of the diffusion of water molecules.

3.6. Mechanical properties.

Table 6 displays the values of TS, EAB, and YM of bare GelA films and GelA/BCNC films incorporating CEO at different concentrations. Bare GelA films exhibited a TS value of ~10 MPa, which is in line with values reported in the literature for fish gelatin. For example, for triggerfish and tilapia fish gelatin Arpi and co-workers found a TS value of 2.34 and 1.72 MPa [52], whereas a TS value of 2.97, 3.21, and 5.57 MPa was found for bovine, porcine, and chicken skin gelatin, respectively [53]. A lower TS value (0.58 MPa) was measured for tilapia bone gelatin [54], whereas Jiang et al. [55] and Lee et al. [56], respectively, measured the highest TS for catfish gelatin (17.3 MPa) and starfish gelatin (19.61 MPa). These differences between TS values have mostly been ascribed to different amino acid composition and geographical origin that, in turn, would affect the gel strength [57]. For instance, gelatin with a lower content of the amino acids proline and hydroxyproline shows lower gel modulus and lower TS values [58].

As shown in Table 6, CEO/GelA-BCNC emulsion films exhibited lower TS, higher EAB, and lower YM compared to bare GelA films. This behavior in not surprising if we consider that CEO acted as a plasticizer, that is, it increased the intermolecular free volume within the main gelatin network, thus hindering the hydrogen bonding pattern of native gelatin [59]. From a practical point of view, these results demonstrated that the addition of CEO lowered the inherent brittleness of gelatin films, allowing to avoid the use of conventional plasticizers (e.g., glycerol, sorbitol, etc.).

4. Conclusions

Films made from cinnamon essential oils encapsulated in nanodroplets of fish gelatin and bacterial cellulose nanocrystals were here tested as a potential matrix for the generation of controlled-release packaging systems—e.g., in the form of coatings deposited directly on the food surface or on the inner side of packaging films (i.e., the side facing the food). This investigation showed that the encapsulation of the active compound (CEO) is a feasible approach to obtain a sustained release over time while achieving other functional properties such as optical clearance and surface hydrophobicity. In addition, the assessment of the barrier performance of films against oxygen, carbon dioxide, and water vapor suggested the potential of CEO/GelA-BCNC films for the shelf life extension of living foods, such as MAP-packaged crustaceans and mollusks as well as fruits and vegetables. In vivo experiments including antimicrobial tests on real foods and sensory tests are the next steps to confirm the practical use of this solution.

Acknowledgments

Mahsa Razavi is grateful to the Ministry of Science, Research and Technology of Iran for financial support during her stay at the University of Milan.

Authors' Contributions

Conceptualization: M.R. and S.F.; methodology, M.R. and S.F.; formal analysis, M.R., C.R. and S.F.; writing—original draft preparation, M.R.; writing—review and editing, M.R., A.G., A.N. and S.F.; visualization, S.F.; supervision, S.F. All authors have read and agreed to the published version of the manuscript.

Conflict of Interest

The authors declare that they have no known competing financial interests or personal relationships that could have appeared to influence the work reported in this paper.

References

1. K. Nilsuwan, S. Benjakul, T., Food Biophys. **12**, 234–243 (2017). https://doi.org/10.1007/s11483-017-9479-2

2. S. Mangaraj, A. Yadav, L. M. Bal, S. K. Dash, N. K. Mahanti, J. Packag. Technol. Res. **3**, 77–96 (2019). https://doi.org/10.1007/s41783-018-0049-y

3. C. L. Reichert, E. Bugnicourt, M. B. Coltelli, P. Cinelli, A. Lazzeri, I. Canesi, F. Braca, B. M. Martínez, R. Alonso, L. Agostinis, S. Verstichel, L. Six, S. D. Mets, E. C. Gómez, C. Ißbrücker, R. Geerinck, D. F. Nettleton, I. Campos, E. Sauter, P. Pieczyk, M. Schmid, Polymers, **12**, 1558–1593 (2020). https://doi.org/10.3390/polym12071558

4. S. Farris, L. Introzzi, L. Piergiovanni, Packag. Technol. Sci. **22**, 69–83 (2009). https://doi.org/10.1002/pts.826

5. P. Kanmani, J. W. Rhim, Food Hydrocoll. **35**, 644–652 (2014). https://doi.org/10.1016/j.fooyd.2013.08.011

6. P. Tongnuanchan, S. Benjakul, T. Prodpran, S. Pisuchpen, K. Osako, Food Hydrocoll. **56**, 93–107 (2016). https://doi.org/10.1016/j.foodhyd.2015.12.005

7. J.-Y. Zhu, C.-H. Tang, S.-W. Yin, Y.-G. Yu, J.-H. Zhu, X.-Q. Yang, Food Biophys. **12**, 451–461 (2017). https://doi.org/10.1007/s11483-017-9501-8

8. S. F. Hosseini, M. Rezaei, M. Zandi, F. Farahmandghavi, Food Chem., **136**, 1490–1495 (2013). https://doi.org/10.1016/j.foodchem.2012.09.081

9. A. Lu, Z. Ma, J. Zhuo, G. Sun, G. Zhang, J. Appl. Polym. Sci. **128**, 970–975 (2013). https://doi.org/10.1002/app.38131

10. J. F. Martucci, R. A. Ruseckaite, Polym. Degrad. Stabil. **94**, 1307–1313 (2009). https://doi.org/10.1016/j.polymdegradstab.2009.03.018

11. C. Mu, J. Guo, X. Li, W. Lin, D. Li, Food Hydrocolloid **27**, 22–29 (2012). https://doi.org/10.1016/j.foodhyd.2011.09.005

12. C. Peña, G. Mondragon, I. Algar, I. Mondragon, J. Martucci, R. Ruseckaite, in Gelatin: production, applications and health implications, ed. By G. Boran (Nova Publishers, New York, 2013), pp. 71-86

13. W. Wang, Y. Liu, H. Jia, Y. Liu, H. Zhang, Z. He, Y. Ni1, Food Biophys. **12**, 23–32 (2017). https://doi.org/10.1007/s11483-016-9459-y

14. C. Vichasilp, S. Sai-Ut, S. Benjakul, S. Rawdkuen, Food Biophys. **9**, 238–248 (2014). https://doi.org/10.1007/s11483-014-9345-4

15. L. Lin, J. M. Regenstein, S. Lv, J. Lu, S. Jiang, Trends Food Sci. Tech. **68**, 102–112. (2017). https://doi.org/10.1016/j.tifs.2017.08.012

16. S. F. Hosseini, M. Rezaei, M. Zandi, F. Farahmandghavi, Food Chem. **194**, 1266–1274 (2016). http://dx.doi.org/10.1016/j.foodchem.2015.09.004

17. J. Wu, X. Sun, X. Guo, S. Ge, Q. Zhang, Aquac. Fish. **2**, 185–192 (2017). http://dx.doi.org/10.1016/j.aaf.2017.06.004

18. L. Scartazzini, J. V. Tosati, D. H. C. Cortez, M. J. Rossi, S. H. Flôres, M. D. Hubinger, M. Di Luccio, A. R. Monteiro, J. Food Sci. Tech. **56**, 4045–4056 (2019). https://doi.org/10.1007/s13197-019-03873-9

19. P. Tongnuanchan, S. Benjakul, T. Prodpran, Food Chem. **134**, 1571–1579 (2012). doi: 10.1016/j.foodchem.2012.03.094

20. M. S. Razavi, A. Golmohammadi, A. Nematollahzadeh, F. Fiori, C. Rovera, S. Farris, Food Hydrocoll. **109**, 106111–106118 (2020). https://doi.org/10.1016/j.foodhyd.2020.106111

21. Z. Dong, F. Xu, I. Ahmed, Z. Li, H. Lin, Food Control **92**, 37–46 (2018). https://doi.org/10.1016/j.foodcont.2018.04.052

22. S. Sharma, S. Barkauskaite, A. K. Jaiswal, S. Jaiswal, Food Chem. **343**, 128403–128413 (2020). https://doi.org/10.1016/j.foodchem.2020.128403

23. T. L. Cao, K. B. Song, LWT **131**, 109647–109655 (2020). https://doi.org/10.1016/j.lwt.2020.109647

24. C. Rovera, M. Ghaani, N. Santo, S. Trabattoni, R. T. Olsson, D. Romano, S. Farris, ACS Sustain. Chem. Eng. **6**, 7725–7734 (2018). https://doi.org/10.1021/acssuschemeng.8b00600

25. E. V. R. Campos, P. L. F. Proença, J. L. Oliveira, A. E. S. Pereira, L. Nunes de Morais Ribeiro, F. O. Fernandes, K. C. Gonçalves, R. A. Polanczyk, T. Pasquoto-Stigliani, R. Lima, C. C. Melville, J. F. Della Vechia, D. J. Andrade, L. F. Fraceto, Sci. Rep., **8**, 7623 (2018). http://dx.doi.org/ 10.1038/s41598-018-26043-x

26. L. S. Silva, J. M. Mar, S. G. Azevedo, M. S. Rabelo, J. A. Bezerra, P. H. Campelo, M. B. Machado, G. Trovati, A. L. dos Santos, H. D. da Fonseca Filho, D. P. de Souza, E. A. Sanches, J. Sci. Food Agr. **99**, 685–695 (2018). https://doi.org/10.1002/jsfa.9233

27. European Commission. (2011). Commission Regulation (EU) No 10/2011 of 14 January 2011 on plastic materials and articles intended to come into contact with food. In European Commission (Ed.) *Official Journal of the European Union* (pp. 1–89)

28. D. Natrajan, S. Srinivasan, K. Sundar, A. Ravindran, J. Food Drug Anal. **23**, 560–568 (2015). http://dx.doi.org/10.1016/j.jfda.2015.01.001

29. K. H. Ramteke, P. A. Dighe, A. R. Kharat, S. V. Patil, Scholars Academic Journal of Pharmacy **3**, 388–396 (2014)

30. H. K. Shaikh, R. V. Kshirsagar, S. G. Patil, World Journal of Pharmacy and Pharmaceutical Sciences **4**, 324–338 (2015)

31. I.U. Unalan, D. Boyaci, S. Trabattoni, S. Tavazzi, S. Farris, Nanomaterials **7**, 281 (2017). https://doi.org/10.3390/nano7090281

32. C. A. Cozzolino, G. Castelli, S. Trabattoni, S. Farris, Food Packag. Shelf Life **8**, 50–55 (2016). http://dx.doi.org/ 10.1016/j.fpsl.2016.03.003

33. M. L. Bruschi, in Strategies to Modify the Drug Release from Pharmaceutical Systems, ed. By M. L. Bruschi (Woodhead Publishing, Cambridge, 2015), pp. 63–86. https://doi.org/10.1016/B978-0-08-100092-2.00005-9

34. S. Dash, P. N. Murthy, L. Nath, P. Chowdhury, Acta Pol. Pharm. **67**, 217–223 (2010).

35. D. R. Paul, Int. J. Pharmaceut. **418**, 13–17 (2011). https://doi.org/10.1016/j.ijpharm.2010.10.037

36. N. Mhlanga, S. Sinha Ray, Int. J. Biol. Macromol. **72**, 1301–1307 (2015). https://doi.org/10.1016/j.ijbiomac.2014.10.038

37. N. A. Peppas, Pharm. Acta Helv. **60**, 110–111 (1985)

38. J. Xu, B. Xu, D. Shou, X. Xia, Y. Hu, Polymers **7**, 1850–1870 (2015). http://dx.doi.org/10.3390/polym7091488

39. H. Rezaeinia, B. Ghorani, B. Emadzadeh, N. Tucker, Food Hydrocoll. **93**, 374–385 (2019). https://doi.org/10.1016/j.foodhyd.2019.02.018

40. M. Mehran, S. Masoum, M. Memarzadeh, Ind. Crop. Prod. **154**, 112694–112702 (2020). https://doi.org/10.1016/j.indcrop.2020.112694

41. R. F. Da Silva Barbosa, E. Della Coletta Yudice, S. K. Mitra, D. Dos Santos Rosa, Food Control **121**, 107605–107613 (2021). https://doi.org/10.1016/j.foodcont.2020.107605

42. F. Xue, Y. Gu, Y. Wang, C. Li, B. Adhikari, Food Hydrocoll. **96**, 178–189 (2019). https://doi.org/10.1016/j. foodhyd.2019.05.014

43. J. Wu, H. Liu, S. Ge, S. Wang, Z. Qin, L. Chen, Q. Zheng, G. Liu, G. Zhang, Food Hydrocoll. **43**, 427–435 (2015). http://dx.doi.org/10.1016/j.foodhyd.2014.06.017

44. C. A. Cozzolino, G. Campanella, H. Türe, R. T. Olsson, S. Farris, Carbohydr. Polym. **143**, 179–187 (2016). http://dx.doi.org/10.1016/j.carbpol.2016.01.068

45. Y. Yao, D. Ding, H. Shao, Q. Peng, Y. Huang, Int. J. Polym. Sci. **2017**, 1–9 (2017). https://doi.org/10.1155/2017/1837171

46. I.U. Unalan, C. Wan, L. Figiel, R. T. Olsson, S. Trabattoni, S. Farris, Nanotechnology **26**, 275703–275713 (2015). https://doi.org/10.3390/nano10040735

47. D. Boyaci, G. Iorio, G. S. Sozbilen, D. Alkan, S. Trabattoni, F. Pucillo, S. Farris, A. Yemenicioğlu, Food Packag. Shelf Life **20**, 100316–100326 (2019). https://doi.org/1016/j.fpsl.2019.100316

48. X. Li, X. Yang, H. Deng, Y. Guo, J. Xue, Int. J. Biol. Macromol. **150**, 161–168 (2020). https://doi.org/10.1016/j.ijbiomac.2020.02.066

49. C. Rovera, H. Türe, M. S. Hedenqvist, S. Farris, Food Packag. Shelf Life **26**, 100561–100572 (2020). https://doi.org/10.1016/j.fpsl.2020.100561

50. G. Mondragon, C. Peña-Rodriguez, A. Gonzalez, A. Eceiza, A. Arbelaiz, Eur. Polym. J. **62**, 1–9 (2015). https://doi.org/10.1016/j.eurpolymj.2014.11.003

51. N. M. D'Cruz, L. N. Bell, J. Food Sci. **70**, 64–68 (2006). https://doi.org/10.1111/j.1365-2621.2005.tb07092.x

52. N. Arpi, F. Martunis, E. Hardianti, IOP Conf. Ser.: Earth Environ. Sci. **207**, 012050 (2018). https://doi.org/10.1088/1755-1315/207/1/012050

53. N. Suderman, M.I.N. Isa, N.M. Sarbon, IOP Conf. Ser.: Mater. Sci. Eng. **440**, 012033 (2018). https://doi.org/10.1088/1757-899x/440/1/012033

54. W. Atmaka, B. Yudhistira, M.I.S. Putro, IOP Conf. Ser.: Earth Environ. Sci. **142**, 012028 (2018). https://doi.org/10.1088/1755-1315/142/1/012028

55. M. Jiang, S. Liu, X. Du, Y. Wang, Food Hydrocoll. **24**, 105–110 (2010). https://doi.org/10.1016/j.foodhyd.2009.08.011

56. K.-Y. Lee, J.-H. Lee, H.-J. Yang, K.B. Song, Food Sci. Biotechnol. **25**, 1023–1028 (2016). https://doi.org/10.1007/s10068-016-0165-9

57. N. Mhd Sarbon, F. Badii, N.K. Howell, Food Hydrocoll. **30**, 143–151 (2013). https://doi.org/10.1016/j.foodhyd.2012.05.009

58. Z. A. Nur Hanani, Y. H. Roos, J.P. Kerry, Int. J. Biol. Macromol. **71**, 94–102 (2014). https://doi.org/10.1016/j.ijbiomac.2014.04.027

59. J. Wu, H. Liu, S. Ge, S. Wang, Z. Qin, L. Chen, Q. Zheng, Q. Liu, Q. Zhang, Food Hydrocoll. **43**, 427–435 (2015). https://doi.org/10.1016/j.foodhyd.2014.06.017

Figure captions

Fig. 1 Release profile of CEO from GelA/BCNC nanocapsules (see the main text for details about the code meaning). The release assay was performed by the dialysis membrane bag method at room temperature (23 °C), in ethanol/water solution (20%, w/w)

Fig. 2 Contact angle values recorded for the CEO-GelA/BCNC emulsion films with different amount of CEO (from 0.3 v/w % to 0.48 v/w %)

Figure 1

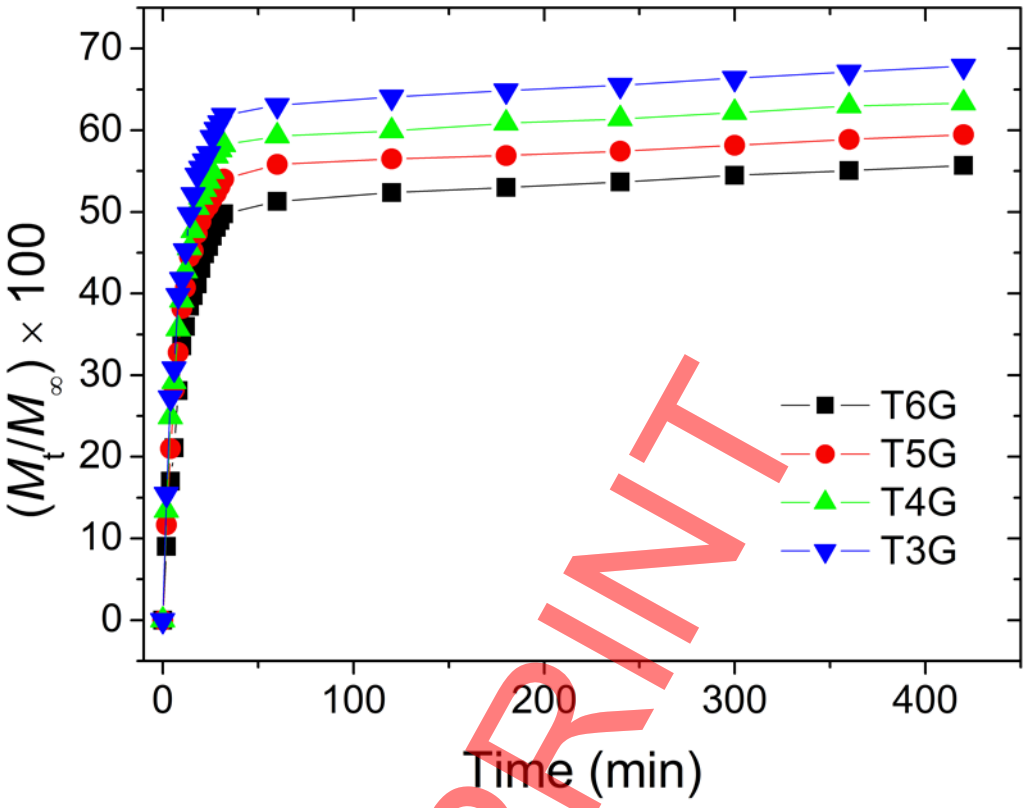

Figure 2

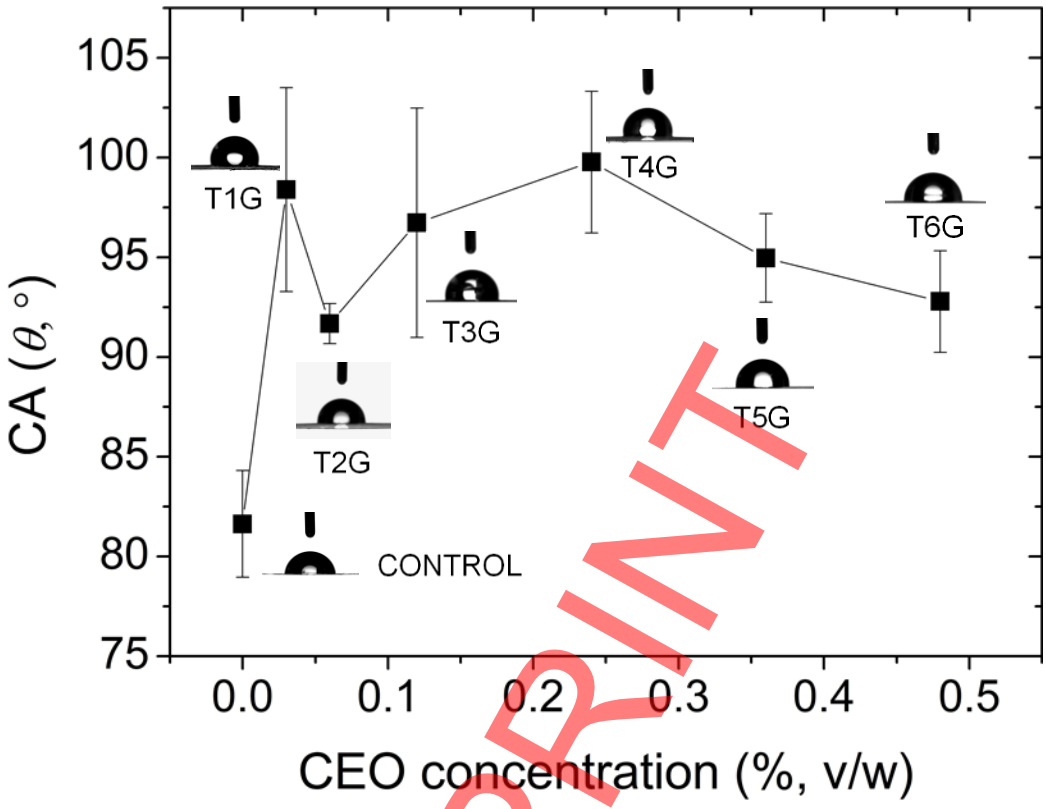

Tables

Table 1 Kinetic models, relevant equations, regression plots, and extracted parameters used to assess CEO release from GelA/BCNC nanocapsules

Kinetic model	Equation	Plot	Parameter
Zero-order	$M_t = M_0 + K_0 t$	$M_t/M_\infty vs\ time$	R^2 K_0
First-order	$log\ M_t = logM_0 + K_1 t$	$log\ (1 - M_t/M_\infty) vs\ time$	R^2 K_1
Higuchi	$M_t = M_0 + K_H t^{1/2}$	$M_t/M_\infty vs\ \sqrt{(time)}$	R^2 K_H
Hixson-Crowell	$\sqrt[3]{M_0} - \sqrt[3]{M_t} = K_{HC} t$	$1 - (1 - M_t/M_\infty)^{1/3}\ vs\ time$	R^2 $K_{1/3}$
Korsmeyer–Peppas	$M_t/M_\infty = K_{KP} t^n$	$log\ (M_t/M_\infty) vs\ log\ (time)$	R^2 K_{KP} n

M_t/M_∞ = fraction of the active compound released

M_0 = initial amount of the active compound loaded into the matrix

M_t = cumulative amount of active compound released at time t (with the exception of Hixon-Crowell equation, where M_t indicates the amount of compound remaining in the matrix at time t)

M_∞ = theoretical cumulative amount of active compound released at infinite time (the maximum released amount found at the plateau of the release curves)

K_0, K_1, K_H, K_{HC}, and K_{KP} = release rate constants

n = release exponent of the Korsmeyer-Peppas model

Table 2 Diffusional interpretation of experimental release data based on the release exponent (n) of the Korsmeyer-Peppas model for polymeric matrices of different shapes

Exponent (n)			Release mechanism
Film	Cylinder	Sphere	
0.5	0.45	0.43	Fickian diffusion
$0.5 < n < 1$	$0.45 < n < 0.89$	$0.43 < n < 0.85$	Anomalous transport
1.0	0.89	0.85	Case II transport
$1.0 < n$	$0.89 < n$	$0.85 < n$	Super case II transport

Adapted from Mhlanga and Sinha Ray (2015).

Table 3 Release rate constants (K), correlation coefficients (R^2), and n exponent calculated by fitting the experimental release data of CEO from the GelA/BCNC emulsions (pH 5) with five different mathematical models

CEO-GelA/BCNC formulation	Equation type and modelling parameters										
	Zero-order		First-order		Higuchi		Hixson-Crowell		Korsmeyer-Peppas		
	K_0	R^2	K_1	R^2	K_H	R^2	K_{HC}	R^2	K_{KP}	n	R^2
T3G	0.040	0.930	-0.023	0.995	0.137	0.986	0.016	0.952	0.105	0.621	0.975
T4G	0.038	0.941	-0.021	0.969	0.127	0.987	0.015	0.961	0.089	0.659	0.977
T5G	0.037	0.968	-0.021	0.987	0.122	0.979	0.012	0.982	0.072	0.733	0.993
T6G	0.033	0.987	-0.017	0.960	0.105	0.956	0.015	0.993	0.052	0.802	0.994

Table 4 Thickness, total light transmittance, and haze of CEO-BCNC/GelA active films prepared at pH 5 and loaded with different CEO concentrations

Treatments	Thickness (µm)	Total transmittance (%)	Haze (%)
Control	28.3 ± 1.63[a]	90.84 ± 0.2[a]	0.96 ± 0.01[a]
T1G	31.83 ± 2.78[a]	90.82 ± 0.6[a]	0.98 ± 0.02[a]
T2G	29.7 ± 2.83[a]	90.65 ± 0.9[a]	1.02 ±0.02[a]
T3G	33.6 ± 4.45[a]	90.47 ± 0.8[a]	1.03 ± 0.03[a]
T4G	29.8 ± 3.08[a]	90.41 ± 0.7[a]	1.15 ± 0.02[b]
T5G	30.33 ± 1.03[a]	90.22 ± 0.8[a]	1.9 ± 0.02[c]
T6G	30.78 ± 2.55[a]	89.95 ± 0.5[a]	2.38 ± 0.03[d]

Roman superscripts denote statistically significant differences ($p < 0.05$) within a group.

Table 5 Oxygen, carbon dioxide, and water vapor transmission rates of films incorporated with CEO concentrations of 0.12 v/w % and 0.24 v/w %

Treatments	O_2TR [$cm^3/(m^2\ 24h)$]		CO_2TR [$cm^3/(m^2\ 24h)$]		WVTR [$g/(m^2\ 24h)$]
	0% RH	50% RH	0% RH	50% RH	50% RH
T3G	19.9 ± 2.9^{a}	2074.2 ± 255.3^{c}	822.6 ± 71.8^{e}	> DL	288.8 ± 11.5^{g}
T4G	74.3 ± 6.7^{b}	24771.8 ± 1982.2^{d}	2260.4 ± 205.6^{f}	> DL	264.1 ± 9.2^{h}

Roman superscripts denote statistically significant differences ($p < 0.05$) within a group.

*Recorded values are above the upper detection limit of the instrument.

Table 6 Tensile strength (TS), elongation at break (EAB), and Young's modulus (YM) of bare fish gelatin films and CEO-GelA/BCNC emulsion films

CEO Concentrations (μL/L)	TS (MPa)	EAB (%)	YM (Pa)
0	10.16 ± 0.32^{a}	0.985 ± 0.14^{c}	337.56 ± 9.36^{a}
1200	8.724 ± 0.89^{b}	1.34 ± 0.38^{c}	305.42 ± 18.41^{ab}
1800	4.964 ± 0.92^{c}	1.945 ± 0.27^{b}	247.67 ± 59.43^{bc}
2400	3.105 ± 0.60^{d}	3.197 ± 0.3^{a}	237.68 ± 28.11^{c}

Roman superscripts denote statistically significant differences ($p < 0.05$) within a group.

Graphical Abstract